

AD-A202 380

FILE COPY

4

OFFICE OF NAVAL RESEARCH

PUBLICATIONS/PATENTS/PRESENTATIONS/HONORS REPORT

for

October 1, 1987 through September 30, 1988

for

Contract N00014-87-K-0243

R&T #414e340

Materials Processing of Diamond:  
Etching, doping by Ion Implantation and Contact Formation

Wei-Kan Chu  
University of North Carolina  
Department of Physics & Astronomy  
CB#3255 Phillips Hall  
Chapel Hill, NC 27599-3255

DTIC  
ELECTE  
NOV 17 1988  
S D  
CH

Reproduction in whole, or in part, is permitted for any purpose of the United States Government.

This document has been approved for public release and sale; its distribution is unlimited.

88 11 17 008

a. Papers submitted and not yet published

G.S. Sandhu, M.L. Swanson, and W.K. Chu, "Doping of Diamond by Ion Implantation," to be published in the Proceedings of the 32nd SPIE Symposium, San Diego, CA, Aug. 1988.

W.K. Chu, G.S. Sandhu, N.R. Parikh, M.L. Swanson, C. Childs, J.M. Mikrut, and L.E. McNeil, "Characterization of diamond-like films," to be published in the Proceedings of the 32nd SPIE Symposium, San Diego, CA, Aug. 1988.

b. Papers published

(none)

c. Books submitted for publications

(none)

d. Books published

(none)

e. Patents filed

(none)

f. Patents granted

(none)

g. Invited presentations

G.S. Sandhu, M.L. Swanson, and W.K. Chu, "Doping of Diamond by Ion Implantation," 32nd SPIE Symposium, San Diego, CA, August 14-19, 1988.

W.K. Chu, G.S. Sandhu, N.R. Parikh, M.L. Swanson, C. Childs, J.M. Mikrut, and L.E. McNeil, "Characterization of diamond-like films," 32nd SPIE Symposium, San Diego, CA, August 14-19, 1988.

J.F. Prins, "A Real Cool Way to Dope Diamonds," Naval Research Laboratory, Electronics Science & Technology Division, August 25, 1988.

h. Contributed presentations

W.K. Chu, "Ion Implantation of Boron in Diamond," IBMM'88 Conference, June 12-17, 1988, Tokyo, Japan.

G.S. Sandhu, M.L. Swanson, and W.K. Chu, "Doping of Diamonds by Ion Implantation," Diamond Technology Initiative Symposium, July 12-14, 1988 Crystal City, Va.



For	<input checked="" type="checkbox"/>
	<input type="checkbox"/>
	<input type="checkbox"/>
on	
n/	
ty Codes	
and/or	
Special	

A-1

i. Honors, awards, prizes

Wei-Kan Chu, PI: recipient of a Senior U.S. Scientist Award  
(the Alexander von Humboldt Award), 1988.

j. Graduate Students and Post-doctorals supported

Graduate Students:

G. Sandhu  
B. Liu (Summer)  
D. Thompson (Summer)  
J. Austin (Summer)

OFFICE OF NAVAL RESEARCH

1 October 1987 through 30 September 1988

Contract N00014-87-K-0243

R&T No 414e340

ANNUAL TECHNICAL REPORT

Materials Processing of Diamond:  
Etching, Doping by Ion Implantation and Contact Formation

Wei-Kan Chu, Principal Investigator  
Department of Physics & Astronomy  
University of North Carolina  
Chapel Hill, NC 27599-3255

(919) 962-3014

Reproduction in whole, or in part, is permitted for any purpose of the United States Government.

This document has been approved for public release and sale; its distribution is unlimited.

## I. INTRODUCTION

We have made progress on our diamond research program in several areas.

1. Doping of Natural Diamonds
2. Adhesion of Metal Film on Diamond
3. Etching of Diamond surface
4. Characterization of diamond-like films.

We will briefly describe the above items here and attach preprints in appendix to this report.

## II. DOPING OF NATURAL DIAMOND

We have doped natural diamond with B or P ion implantation at liquid nitrogen temperature. Ions of C were implanted prior to the dopant implants, in order to enhance the vacancy concentration in the diamond, thereby increasing the likelihood that the dopant atoms would occupy substitutional lattice sites, and thus be electrically active. Various post-implantation annealing methods were employed to reduce the residual damage in the crystals.

Type IIa diamond crystals were implanted with boron ions with or without prior carbon ion implantation. The samples were kept at liquid nitrogen temperature during both implantation steps. A strong near-edge optical absorption band appeared after implantation, and partially recovered during annealing at 800 °C. For the highest B implantation fluence, optical absorption peaks at 2800 to 3000  $\text{cm}^{-1}$  were observed that were in the same vicinity as the absorption peaks attributed to substitutional boron atoms in natural p-type diamond. Electrical measurements for three of the samples demonstrated well-defined activation energies that could be associated with hopping conduction and/or activation of B dopant atoms. This work shows that p-type doping in diamond by boron ion implantation is feasible, using a suitable combination of low temperature implantation and subsequent annealing.

The complete paper of the B implantation results, presented at the SPIE Diamond Optics Symposium (to be published) is given in Appendix 1.

1000

### III. ADHESION OF METAL ON DIAMOND SURFACES

The chemical inertness of diamond causes poor adhesion of metal films to diamond. This problem is particularly acute with gold films which are of considerable interest since they have potential use in electrodes when using diamonds for microelectronic applications, as well as for mechanical attachment of diamonds to various other metals and alloys.

In the past, the problem of attaching gold films to diamond was partially solved, for limited applications, by having a refractory metal film, such as tungsten, tantalum, or titanium, between the diamond and the gold. The bonding of the refractory metal to the diamond takes place by heating the diamond at several hundred degrees centigrade. Even the heat treatment does not always produce a mechanically stable bond between the diamond and the metal films.

We have developed procedures for improving the adhesion of gold to diamond without any heat treatment.

This report includes the results of two experiments designed to test the change in gold adhesion to diamond by ion mixing after deposition of the gold and by argon sputtering prior to deposition of the gold film. (*Appendix 4*)

### IV. ETCHING

Reliable means of removing surface layers of diamond have been developed. Oxygen plasma etching at 30nm/min gives very reproducible results. Our etching studies are documented in Appendix 3.

### V. CHARACTERIZATION OF DIAMOND-LIKE FILMS

Thin diamond-like and diamond films, grown by remote plasma-enhanced CVD (RPECVD) and by plasma CVD, were characterized using optical microscopy, elastic recoil detection spectroscopy (ERD), and Raman scattering. The films were supplied by the Research Triangle Institute, by Crystallume Corp. and by General Electric Co. The H concentration of the films was measured by ERD and

was related to the growth parameters and to the quality of the films as determined by Raman scattering.

The H content of samples grown by RPECVD at the Research Triangle Institute increased with decreasing growth temperature, varying from 6 at% H at growth temperatures from 500-720°C, to 25 at% H at a growth temperature of 20°C. The characteristic Raman frequency of natural diamond,  $1332\text{ cm}^{-1}$ , was observed for samples grown by Crystallume Corp. and by General Electric Co. The samples obtained from Crystallume showed circular "bull's-eye" features by optical microscopy, and the width of the  $1332\text{ cm}^{-1}$  peak was broad, indicating highly strained crystallites. For a sample from G.E., most of the film was good quality diamond, as indicated by a sharp  $1332\text{ cm}^{-1}$  diamond frequency; the bottom (substrate) part of the film contained more H than the top part. The laser cutting procedure used for preparation of the G.E. films caused a graphitization near the cut surface.

These data demonstrate the usefulness of applying optical, Raman scattering and ion beam analysis methods to the characterization of diamond films, and show that the hydrogen content of these films can be very large.

These results were presented in more detail at the SPIE Diamond Symposium (San Diego, Aug, 1988), and will be published in their proceedings. The paper is included here as Appendix 2.

## VI. APPENDIX

1. Preprint of SPIE-88 talk "A study of the doping process in Diamond by Boron Implantation," G.S. Sandhu, W.K. Chu, M.L. Swanson, and J.F. Prins.
2. Preprint of SPEI-88 talk "Characterization of diamond-like films," N.R. Parikh, W.K. Chu, G.S. Sandhu, M.L. Swanson, C. Childs, J.M. Mikrut, and L.L. McNeil.
3. "Plasma-assisted etching of Diamond," W.K. Chu and G. Sandhu.
4. "Increase in gold-diamond adhesion by argon sputtering of diamond." A preliminary lab report prepared by C. Childs.

A Study of the Doping Process in Diamond  
by Boron Implantation

G.S. Sandhu, W.K. Chu, M.L. Swanson, and J.F. Prins\*  
University of North Carolina, Dept. of Physics & Astronomy  
Chapel Hill, North Carolina 27599-3255  
and  
M.W. Geis,  
MIT Lincoln Laboratory, Lexington, MA 02173

ABSTRACT

Type IIa diamond crystals were implanted with boron ions with or without prior carbon ion implantation. The samples were kept at liquid nitrogen temperature during both implantation steps. A strong near-edge optical absorption band appeared after implantation, and partially recovered during annealing at 800 °C. For the highest B implantation fluence, optical absorption peaks at 2800 to 3000  $\text{cm}^{-1}$  were observed that were in the same vicinity as the absorption peaks attributed to substitutional boron atoms in natural p-type diamond. Electrical measurements for three of the samples demonstrated well-defined activation energies that could be associated with hopping conduction and/or activation of B dopant atoms. This work shows that p-type doping in diamond by boron ion implantation is feasible, using a suitable combination of low temperature implantation and subsequent annealing.

\*Permanent address: University of the Witwatersrand, Johannesburg, South Africa.

## 1. INTRODUCTION

Recent successes in diamond film growth and the possibility of diamond-based microelectronics have triggered a flurry of activity in diamond research.<sup>1</sup> Ion implantation seems to be one of the most promising ways of introducing dopant atoms into diamonds. Attempts to dope diamond by ion implantation have had a long history.<sup>2</sup> Unfortunately, due to the scarcity of diamond samples, most of the early experiments were seldom reproduced. Many of the original claims were intuitively sound but not empirically verified.

Vavilov et al., established at an early stage that electrical conductivity can be obtained by ion implantation.<sup>2,3</sup> They reported that boron or aluminum implanted diamonds were p-type while lithium, carbon and phosphorous implanted diamonds were n-type. Due to the difficulty of making ohmic contacts in the early days, the A.C. conductivities were measured by the microwave method. They also claimed that Hall measurements of boron-implanted diamonds showed a p-type behavior<sup>4</sup> and that p-n junctions could be obtained by boron plus phosphorous implantations.<sup>5</sup> However, complications with interpretation do exist because the intrinsic radiation defects in diamond are also electrically active and may even cause impurity band conduction by means of the hopping mechanism.<sup>6-8</sup>

Diamond is a metastable form of carbon. Thermodynamically, annealing of ion-damaged diamond will thus favor graphite formation unless the kinetics of the process can prevent the transition. Hot implantation was proposed in the hope that dynamic annealing would occur during the implantation process.<sup>9,10</sup> Although graphitization can be prevented in this manner, a dense dislocation network results caused by the interaction of the migrating point defects.<sup>11</sup>

At lower temperatures, where this dynamic annealing does not occur, implantation causes volume expansion. Maby et al.,<sup>12</sup> reported expansion of diamond after boron ion implantation at room temperature and concluded that this was caused by the reduction of material density needed for amorphous carbon formation in diamond. Volume

expansion of diamond measured during ion implantation at different temperatures was studied by Prins et al.<sup>13,14</sup> They observed that no volume expansion could be detected for implantation at liquid nitrogen temperature up to a threshold dose of  $6 \times 10^{15}$  ions/cm<sup>2</sup>.<sup>14</sup> This low temperature result contrasts sharply from ion implantation carried out above room temperature when the expansion occurred already at the onset of ion implantation.<sup>13</sup> The latter volume expansion was attributed to the outdiffusion of carbon interstitials from the ion damaged region, leaving behind a high density of immobile vacancies. In contrast, for implantation at liquid nitrogen temperature, the carbon interstitials as well as the vacancies in the vicinity of the damaged area are immobile.

The above observations are crucial for implantation doping and led Prins<sup>15</sup> to devise a model and strategy which demonstrated that controlled doping of diamond by means of ion implantation can be achieved. According to the recipe, ion implantation should be carried out at a low enough target temperature (for example, liquid nitrogen temperature) to inhibit diffusional motion of the point defects created during the process. This is followed by a suitable annealing cycle which then enhances the probability of dopant-vacancy combination owing to the large defect density. The efficiency of this annealing process should improve when increasing the initial point defect density "frozen" in during cold implantation. This density can be increased relative to the implanted dopant atom density by implantation of, for example, carbon ions.<sup>15</sup> However, the density should be below the threshold value at which the layer will expand to form graphite.<sup>14</sup> In a follow-up paper, Prins<sup>16</sup> also demonstrated that the annealing efficiency can be greatly improved by heating the diamond rapidly to a higher temperature than used for his initial studies. Obviously, the efficiency of this doping process can be improved by optimizing the implantation parameters and the subsequent annealing cycle.

Preliminary experimental results which were obtained when implanting diamond with boron plus carbon ions at low temperature according to the recipe discussed above, are presented in this

paper. This constitutes a report on the ongoing progress of our research on this subject.

## 2. EXPERIMENTAL

Type II-A insulating [110] single crystal diamonds of  $4 \times 4 \times 1 \text{ mm}^3$  (purchased from Dubbeldee Diamond Company) were cleaned in hot chromic acid prior to implantation. The boron implants were done with and without prior carbon implantation at liquid nitrogen temperature. When the double species (C and B) were implanted, the diamond samples were kept cold and inside the implanter without breaking the vacuum. The energy and dose of the implants are summarized in Table I. The implantation energies were selected to match the range of boron ions with that of the vacancy distribution produced by the previous carbon

TABLE I

SAMPLE	IMPLANTED ION	ENERGY (keV)	DOSE (atoms/cm <sup>2</sup> )
1	B	65	$1 \times 10^{14}$
2	C	110	$1 \times 10^{14}$
followed by	B	65	$1 \times 10^{14}$
3	C	200	$3 \times 10^{15}$
followed by	B	120	$1 \times 10^{15}$
4	C	200	$3 \times 10^{14}$
followed by	B	120	$3 \times 10^{15}$
5	C	200	$3 \times 10^{14}$
followed by	B	120	$1 \times 10^{15}$

implantation. This was achieved with the help of computer simulations using the TRIM-88 program.<sup>17</sup> The probability of boron atoms occupying vacant sites in the lattice is expected to be enhanced during ion irradiation and post implant annealing if most of the boron atoms are in the vacancy-rich region. All the implantations were done at liquid nitrogen temperature and the samples were then brought slowly to room temperature. After implantation, some of the diamonds were subjected to isochronal annealing in vacuum ( $5 \times 10^{-6}$  Torr). Rapid thermal annealing (RTA) was also done.

Optical measurements were made at room temperature in the transmission mode using a Nicolet 20DXB FT-IR Spectrophotometer. The optical spectra of all the diamonds were measured before and after ion implantation and after subsequent annealing.

On sample 4, electrically active regions which penetrated through to the implanted layer were made by laser irradiation of the diamond surface to produce a heavily damaged region, and contacts were then made with spring loaded tungsten probes. The current injection into the diamond between two contacts was typically between -100 and +100 nA when the voltage readout covered the region between -5 volts and +5 volts. The resistance R was obtained from the slope of the V vs I trace near the origin. The sample was mounted on a heater and the measurements were made at temperature between 36°C and 300°C.

The samples 3 and 5 were annealed at 900°C for 1 hour and rapid thermal annealed (RTA) at 1100°C for 2 minutes. Optical measurements were then made on these samples and contacts for electrical measurements made by overdoping the contact surfaces.<sup>18</sup> The resistance of these samples was then measured as a function of temperature between 20°C and 300°C.

### 3. RESULTS

The results of the optical measurements are shown in Figs. 1 and 2. Figure 1 shows the absorption spectra in the UV-VIS region for sample 1 (implanted with 65 keV B to a dose of  $10^{14}$  B/cm<sup>2</sup>) after

annealing at different temperatures for 45 minutes. It shows the absorption band (GR-I)<sup>19,20</sup> caused by implantation damage. The gradual annealing of the radiation damage is indicated by the decreasing absorption of the GR-I band and a more dramatic upward movement of the absorption edge at 220nm. It is obvious that the radiation damage was not completely removed even after the 800°C anneal. The step at 800 nm is an artifact due to source and filter change in the instrument.

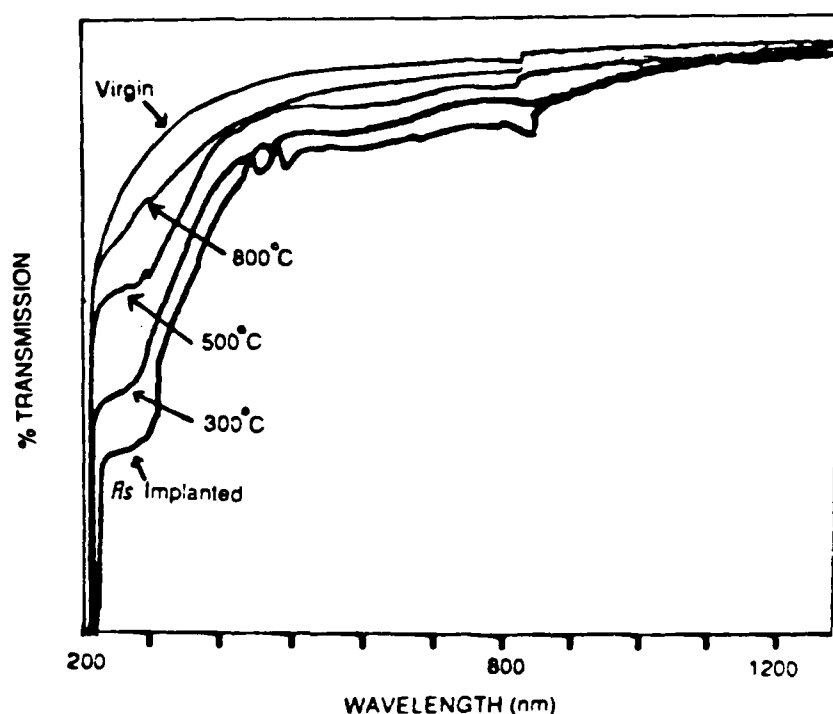


Fig. 1 Optical transmission spectra of diamond implanted with 65 keV boron ions at 77 K to a dose of  $1 \times 10^{14}$  ion per  $\text{cm}^2$  followed by annealing at different temperatures for 45 minutes.

Absorption spectra for sample 4 in the far infrared region are shown in Fig. 2. For comparison, the spectrum obtained from a natural semiconducting diamond containing boron (type IIb) is also shown. After implantation, sample 4 showed two small absorption peaks at  $2957 \text{ cm}^{-1}$  and  $2925 \text{ cm}^{-1}$  (0.365 and 0.361 eV), which were not present before

the implantation. These peaks correspond closely to the position of one of the boron peaks at 0.363 eV observed in the natural semiconducting diamond and it is thus tempting to conclude that the appearance of these peaks indicates the presence of substitutional or near-substitutional boron in the diamond lattice.<sup>21</sup> However, this conclusion must be approached with caution because the dominant peaks at 0.345 eV and 0.305 eV which are always present in natural semiconducting diamond containing boron did not appear after implantation (see Fig. 2). The relative magnitude of the two peaks which are caused by ion implantation into sample 4 was small because

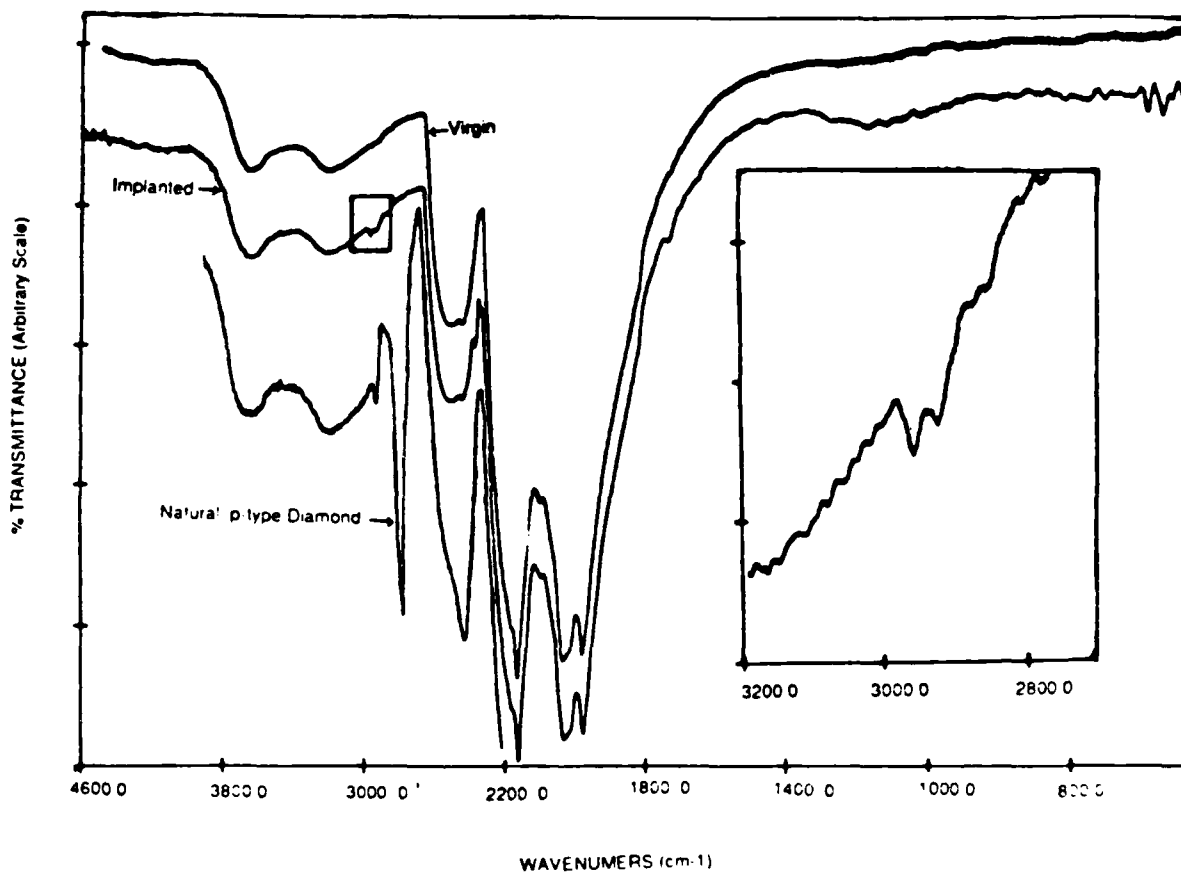


Fig. 2. Absorption spectra for sample 4 (see Table 1) before and after implantation, compared with a spectrum for type IIb diamond. The inset shows the absorption peaks at  $2957\text{ cm}^{-1}$  and  $2925\text{ cm}^{-1}$  for the implanted sample 4.

the thickness of the implanted layer was a minute fraction of the total thickness traversed by the probing beam. It was concluded that in the first two cases of Table I, the boron ion dose could have been too small to cause observable peaks at the same position as seen in sample 4. Unfortunately, samples 3 and 5 already displayed the same peaks before ion implantation and no conclusion could thus be drawn from these measurements. If the peaks were, in these cases, enhanced by the implanted boron, the effect was too small to be measured. It is interesting to note that these peaks can be present in unimplanted, natural diamonds which have been classified as insulating (type IIa).

Because the peaks appeared in sample 4 directly after ion implantation, it was decided to characterize the implanted layer electrically without annealing the diamond. A plot of resistance vs  $1/T$ , given in Fig. 3, yields an activation energy of 0.28 eV, which is

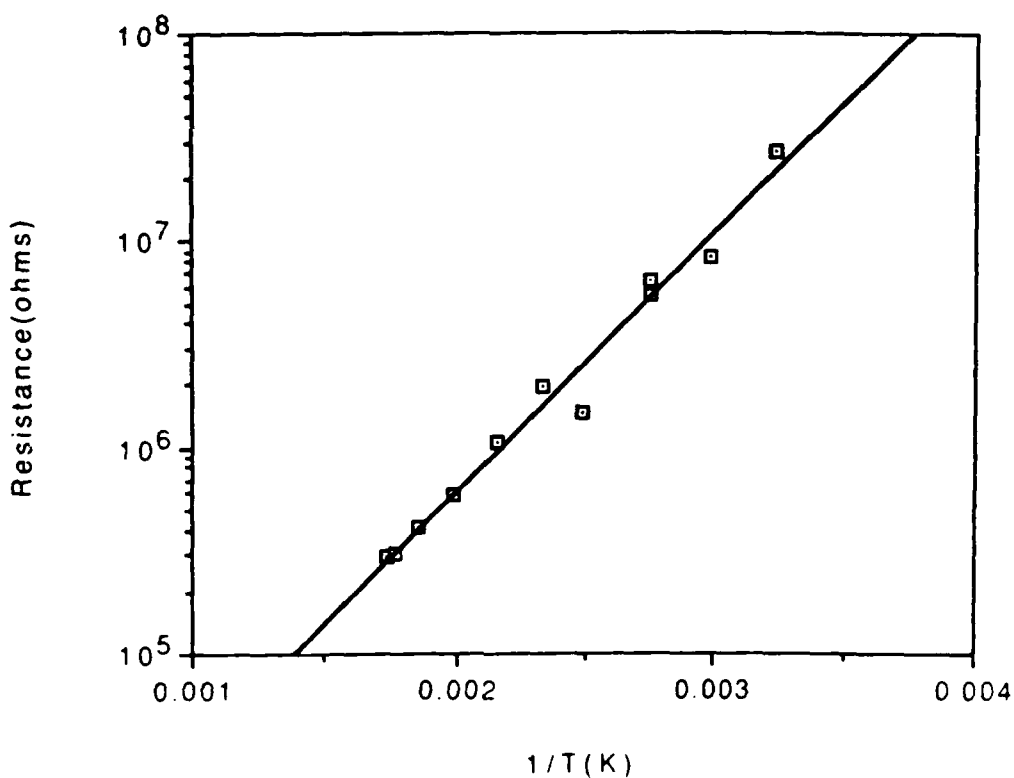


Fig. 3 Electrical resistance versus reciprocal temperature for sample 4 (see Table I) before annealing.

24% below the recognized energy level of substitutional boron in diamond (0.37 eV). This low value, in conjunction with the low resistivities measured, indicates that p-type conductivity by hole activation from boron-acceptors is not the dominating process. The electrical behavior is reminiscent of the initial results which were published by Vavilov et al.<sup>2-5</sup> It would seem logical to conclude that radiation damage rather than substitutional boron is dominating the conduction. This conclusion received further support when this implanted layer turned graphitic after annealing this diamond at 1200°C for 1 hour. Any substitutional boron would have been heavily compensated by the large number of vacancies which act as donors.<sup>22</sup> Thus, if the infra-red absorption peaks which appeared after implanting sample 4 were caused by the presence of substitutional boron, it must be heavily compensated which, in turn, may explain the absence of the other boron peaks which should be there. If this is true, it would mean that samples 3 and 5 already contained compensated substitutional boron before ion implantation. This correlates with the fact that thermally activated conductivity can be measured at high temperatures in type IIa diamonds and that the activation energies seem to be of the correct order of magnitude to explain conduction via hole generation from the charged donors which are compensating boron acceptors.<sup>18</sup>

Samples 3 and 5 were annealed at 900°C for 1 hr and at 1100°C for 2 min using RTA. Neither of the implanted layers graphitized during these anneals. This is a significant result in view of the fact that sample 3 contained more radiation damage (a larger total ion dose) than sample 4 which, as discussed above, graphitized when it was slowly heated and annealed at 1200°C. In the latter case, the residual vacancy density (i.e., the number of vacancies that did not recombine with interstitials) was high enough to induce graphitization. Another noteworthy aspect is that the two small infra-red absorption peaks (at 0.365 and 0.361 eV) which were present in those diamonds and correspond to the peaks which arose in sample 4 after ion implantation, disappeared after RTA. The fact that these peaks were also present in samples 3 and 5 before ion implantation

shows that RTA also caused annealing in virgin, unimplanted diamond.

The conductivity vs  $1/T$  plots for samples 3 and 5 are shown in Fig. 4. Sample 3 showed higher conductivity and a lower activation energy of 0.13 eV at room temperature, whereas sample 5, which received a lower total dose, had lower conductivity and a higher activation energy of 0.2 eV at room temperature which increased to 0.38 eV above 250°C. The four orders of magnitude difference in the conductivities of the two samples may be explained by the higher carbon dose received by sample 3. This will create more vacancies to trap boron atoms in substitutional sites during annealing, resulting

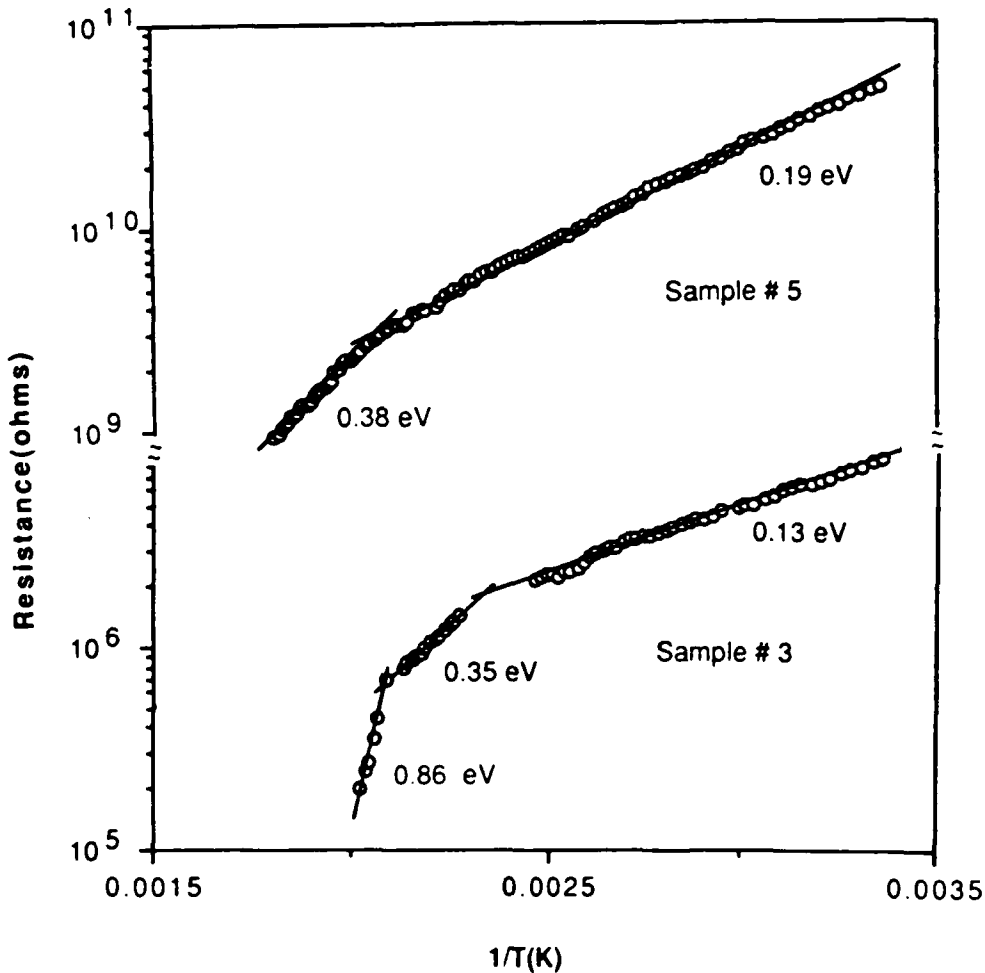


Fig. 4 Electrical resistance versus reciprocal temperature for samples 3 and 5 (see Table I) after 1100°C RTA.

in more efficient doping. On the other hand, the excessive damage produced by these extra carbon ions may also result in higher conductivity after annealing. However, the increase in the slope around 200°C in the case of sample 3 is most probably caused by the interplay between boron acceptors and radiation damage energy levels in diamond, and suggests that there is a significant amount of substitutional boron present in the sample. We expect that the same phenomenon would be observed in the case of sample 5 at higher temperatures.

#### 4. CONCLUSIONS

In summary, doping of diamond by boron ion implantation at low temperature was studied. The diamonds were pre-implanted with carbon in order to increase the doping efficiency. Various post implantation annealing procedures were employed to drive the boron atoms into substitutional sites. These implanted samples were characterized by optical and electrical techniques. It was established that absorption peaks observed in the infrared spectra, which were thought to relate to substitutional boron, could be removed using RTA. The electrical measurements showed features similar to those reported by Prins<sup>16</sup> and indicated the presence of substitutional boron in the implanted samples. The various experimental parameters were by no means optimized because of the limited number of available samples. Nevertheless, the results will be of great assistance in planning future experiments.

#### 5. ACKNOWLEDGEMENTS

This work is supported by the Office of Naval Research contract N00014-87-K-0243. Ion implantation was done in the microelectronics laboratory (North Carolina State University site) of the Microelectronics Center of North Carolina, and optical measurements were done at Research Triangle Institute of North Carolina. We thank M.W. Geis of MIT Lincoln Laboratory, Lexington, MA. for making the electrical measurements for sample 4.

## 6. REFERENCES

1. For example, the Third Annual Diamond Technology Initiative Symposium, July 12-14, 1988, in Arlington, VA has attracted over 60 oral presentations.
2. V.S. Vavilov, M.I. Guseva, E.A. Konorova, V.V. Krasnopevtsev, V.F. Sergienko, and V.V. Tutov, Sov. Phys. Solid State 8, 1560 (1966)
3. V.S. Vavilov, M.I. Guseva, E.A. Konorova and V.F. Sergienko, Sov. Phys. Semiconductor 4, 6 (1970).
4. V.S. Vavilov, M.I. Guseva, E.A. Konorova, and V.F. Sergienko, Sov. Phys. - Semiconductors 4, 12 (1970).
5. V.S. Vavilov, M.A. Gukasyan, M.I. Guseva, E.A. Konorova, and V.F. Sergienko, Sov. Phys. - Doklady 16, 856 (1972).
6. J.J. Hauser and J.R. Patel, Sol. State Comm. 18, 789 (1976).
7. J.J. Hauser, J.R. Patel, and J.W. Rodgers, Appl. Phys. Lett. 30, 129 (1977).
8. R. Kalish, T. Bernstein, B. Shapiro, and A. Talmi, Rad. Eff. 52, 153 (1980).
9. R.S. Nelson, J.A. Hudson, and D.J. Mazey, British patent No 1 476 313, published 10 June 1977.
10. R.S. Nelson, J.A. Hudson, and D.J. Mazey, British patent No 1 599 668, published 7 October 1981.

11. R.S. Nelson, J.A. Hudson, D.J. Mazey, and R.C. Piller, Proc. R. Soc. London A386, 211 (1983).
12. E.W. Maby, C.W. Magee, and J.H. Morewood, Appl. Phys. Lett. 39, 157 (1981).
13. J.F. Prins, T.E. Derry, and J.P.F. Sellschop, Phys. Rev. B34, 8870 (1986).
14. J.F. Prins, T.E. Derry, and J.P. F. Sellschop, Nucl. Instr. & Meth. B18, 261 (1987).
15. J.F. Prins, Phys. Rev. B38, (to be published 1988).
16. J.F. Prins, IBA Conference, April 1988, Johannesburg, South Africa (to be published in Nucl. Instrum. & Methods)
17. J.F. Ziegler, J.P. Biersack, and U. Littmark, The stopping Range of Ions in Solids, Pergamon, New York, 1985.
18. J.F. Prins, to be published.
19. E.C. Lightowers and A.T. Collins (1976). Diamond Research 1976 (Suppl. Ind. Diam. Rev.) pp 14-21.
20. H.B. Dyer and L. du Preez, J. Chem. Phys., 42, 1898 (1965).
21. G.S. Sandhu, M.L. Swanson, and W.K. Chu, IBMM '88, June 12-17, 1988, Tokyo, Japan.
22. H.B. Dyer and P. Ferdinando, Br. J. Appl. Phys. 17, 419 (1966).

## Characterization of diamond-like films

N.R. Parikh, W.K. Chu, G.S. Sandhu, M.L. Swanson,  
C. Childs, J.M. Mikrut and L.E. McNeil

Department of Physics and Astronomy, University of North Carolina  
Chapel Hill, North Carolina 27599-3255

ABSTRACT

Thin diamond-like and diamond films, grown by remote plasma-enhanced CVD (RPECVD) and by plasma CVD, were characterized using optical microscopy, elastic recoil detection spectroscopy (ERD), and Raman scattering. The H concentration of the films was measured by ERD and was related to the growth parameters and to the quality of the films as determined by Raman scattering. The H content of samples grown by RPECVD at the Research Triangle Institute (RTI) increased with decreasing growth temperature, varying from 6 at% H at growth temperatures from 500-720°C, to 25 at% H at a growth temperature of 20°C. The characteristic Raman frequency of natural diamond, 1332  $\text{cm}^{-1}$ , was observed for samples grown by Crystallume Corp. and by General Electric Corp. The samples obtained from Crystallume showed circular "bull's-eye" features by optical microscopy, and the width of the 1332  $\text{cm}^{-1}$  peak was broad, indicating highly strained crystallites. For a sample from G.E., most of the film was good quality diamond, as indicated by a sharp 1332  $\text{cm}^{-1}$  diamond frequency; the bottom (substrate) part of the film contained more H than the top part.

1. INTRODUCTION

Rapid progress has been made in the growth of diamond and diamond-like films by deposition from the vapor phase, using both plasma CVD<sup>1-4</sup> and remote plasma-enhanced CVD<sup>5</sup>. Of special importance for continuing progress in this field is the characterization of

diamond films. In particular, the impurity content of the films is critical, as it can affect both the film integrity and its properties. Since most films are prepared using a  $\text{CH}_4\text{-H}_2$  mixture, the hydrogen content of the films is especially important. We have measured the H concentration of CVD diamond-like films using an ion beam method, elastic recoil detection spectroscopy (ERD). In addition, we have used Raman spectroscopy in a microbeam mode to specify the quality of the diamond-like films as a function of depth, and to relate the film quality to the H content. Ellipsometry (not reported here) and optical microscopy have also been used to characterize the films.

## 2. EXPERIMENTAL PROCEDURE

Samples of diamond or diamond-like films were obtained from RTI, Crystallume and G.E. The films from RTI were grown on Si single crystals by remote plasma enhanced CVD, and the other films were grown by plasma CVD. These samples are not necessarily state-of-the-art or the best films produced by these suppliers; they are however representative examples for demonstration of our characterization methods. The samples were examined by optical and scanning electron microscopy, elastic recoil detection spectroscopy, Raman spectroscopy and ellipsometry.

### 2.1 Elastic recoil detection spectroscopy (ERD)

ERD is a fast and non-destructive method<sup>6</sup> of obtaining H profiles up to depths of about 600 nm. By this method, a beam of MeV energy light ions, for example  $\text{He}^+$ , is directed at the target, causing a small fraction of the H atoms in the target to be ejected by elastic recoil collisions. The concentration of H atoms versus depth in the target can be calculated from the observed energy spectra of the recoiled H atoms, using standard kinematic analysis. The parameters required are the initial energy  $E_0$  of the ion beam, the He-H Rutherford collision cross section  $\sigma$ , the detector solid angle  $\Omega$ , the scattering angle of the recoiled H ions, the energy distribution of the H ions, and the stopping powers  $S_1$  of the incident He ions and  $S_2$

of the recoiled H ions in the target material. Often a standard material containing a known amount of H is used instead of measuring  $\sigma$  and  $\Omega$ .

The concentration  $C_H$  of H atoms in the sample is given by

$$C_H = N(E_H)dE_H / (I\Omega\sigma(E_1)dx), \quad (1)$$

where  $N(E_H)$  is the measured number of recoiled H ions per unit energy,  $dE_H$  is the energy increment corresponding to a depth increment  $dx$ ,  $I$  is the number of incident ions,  $\Omega$  is the detector solid angle and  $\sigma(E_1)$  is the cross section for Rutherford scattering at the incident He energy  $E_1$ .

This technique has a sensitivity of about 0.01 at% H and a depth resolution of about 20 nm. In the present experiments, a beam of 2 MeV  $^4\text{He}^+$  was used, at an incident angle of  $15^\circ$  from the surface, and the recoiled H<sup>+</sup> ions were detected at a forward scattering angle of  $30^\circ$ , as shown in the inset of Fig. 1. The energies of the recoiled H ions were determined by a surface barrier detector which was covered with a  $6\mu\text{m}$  thick Mylar film to shield the backscattered He<sup>+</sup> ions.

## 2.2 Raman Scattering

Raman scattering<sup>7,8</sup> can be used for nondestructive evaluation of the quality of a diamond film, as the dominant zone-center vibrational mode frequencies of diamond ( $1332\text{ cm}^{-1}$ ), graphite ( $1589\text{ cm}^{-1}$ ) and disordered carbon ( $1360\text{ cm}^{-1}$ ) are easily distinguished. The scattering volume examined depends strongly on the penetration depth of the incident light. For incident wavelengths at which the material is transparent the entire thickness can be sampled, but for wavelengths at which it is opaque only the near-surface region can be examined.

Raman scattering measurements were performed using a 0.8 m double-grating spectrometer equipped with photomultiplier detection and photon-counting electronics. Illumination was provided by the

5145 Å line of an Ar<sup>+</sup> laser. The spectral resolution was 1.2 cm<sup>-1</sup> and the polarization of the scattered light was not analyzed.

For coarse measurements conventional focussing optics were used to produce a laser spot size of - 150 μm on the sample. For detailed examination a microscope was used to focus the laser light to a 1.6 μm spot so that features on the sample could be examined at that spatial resolution.

### 3. RESULTS

#### 3.1 RTI Samples

ERD measurements of a diamond-like film grown at 400°C from RTI are shown in Fig. 1. Spectra are given for two different spots on the sample; the different energy widths indicate a 20% variation in film thickness for the two spots. The H concentrations were almost identical for the two spots, as shown by the equal numbers of H counts (the detected number of H recoils). The H concentration profile was obtained directly from the number of H counts versus energy (which is directly proportional to the ERD channel number on the figure), using equation (1). A Mylar film was used as a standard. The H composition was approximately 16 at%, and was almost constant through the film thickness. For RTI films grown at different temperatures, the amount of H in the RTI films decreased with increasing growth temperature, varying from 25 at% for 20°C growth to 6 at% for 500-720°C growth (Table 1).

#### 3.2 Crystallume Samples

ERD results for the Crystallume samples are shown in Fig 2. The films were somewhat thinner than the RTI ones. The H contents for different films are shown in the figure, and varied from 8 at% H to 15 at% H.

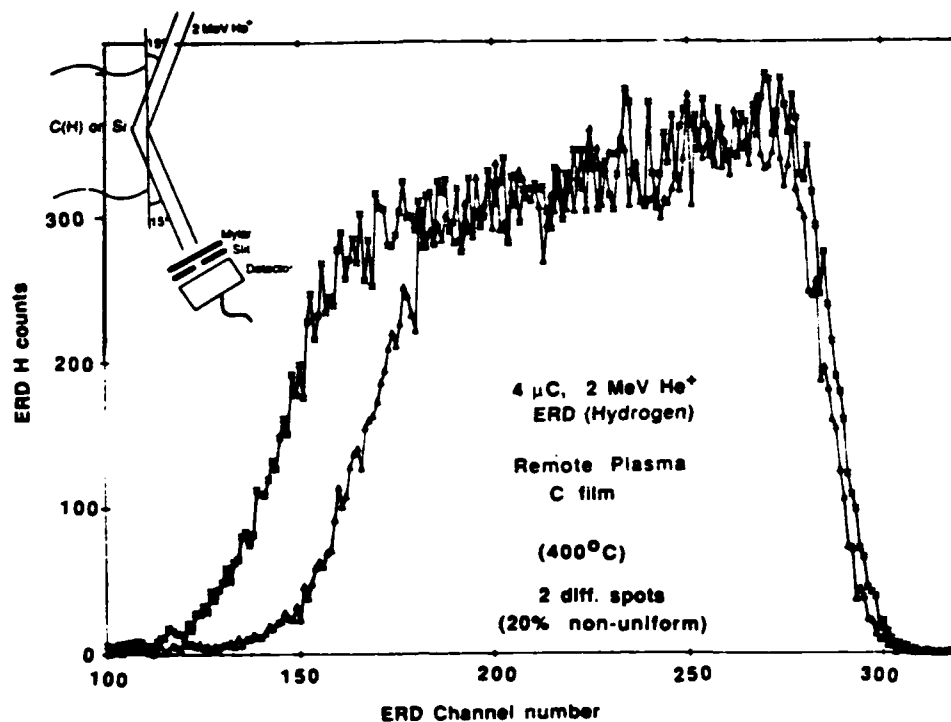


Fig. 1 Elastic recoil spectra recorded at 293K for two different spots on a RTI diamond-like C film, deposited by RPECVD at 400°C on a Si substrate. The incident He<sup>+</sup> energy was 2 MeV. The counted number of recoiled H<sup>+</sup> ions is plotted as a function of their energy (ERD channel number). The inset shows the sample vs detector configuration.

TABLE I

RESULTS OF ERD ANALYSIS OF C(H) FILMS GROWN BY REMOTE PLASMA CVD

Sample Growth Temp. (°C)	C + H (10 <sup>18</sup> /cm <sup>2</sup> )	Layer Thickness (nm) assuming 10 <sup>23</sup> atoms/cm <sup>3</sup>	H/(H+C) (at%)
20	10	100	25
400	4.0	40	16
500	3.3	33	6
600	0.7	7	
650			7.5
720			4.2

Fig. 2. Elastic recoil spectra for Crystallume samples, recorded as in Fig. 1. The three spectra were obtained for different samples.

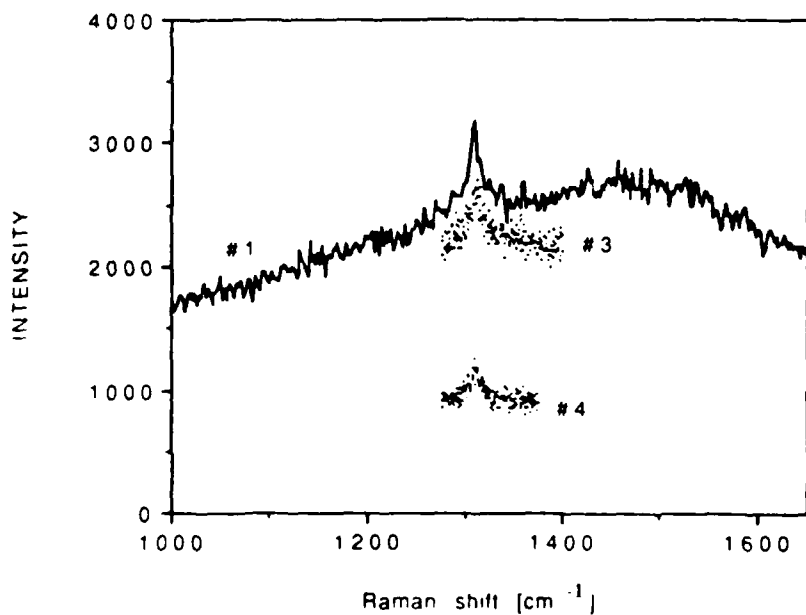
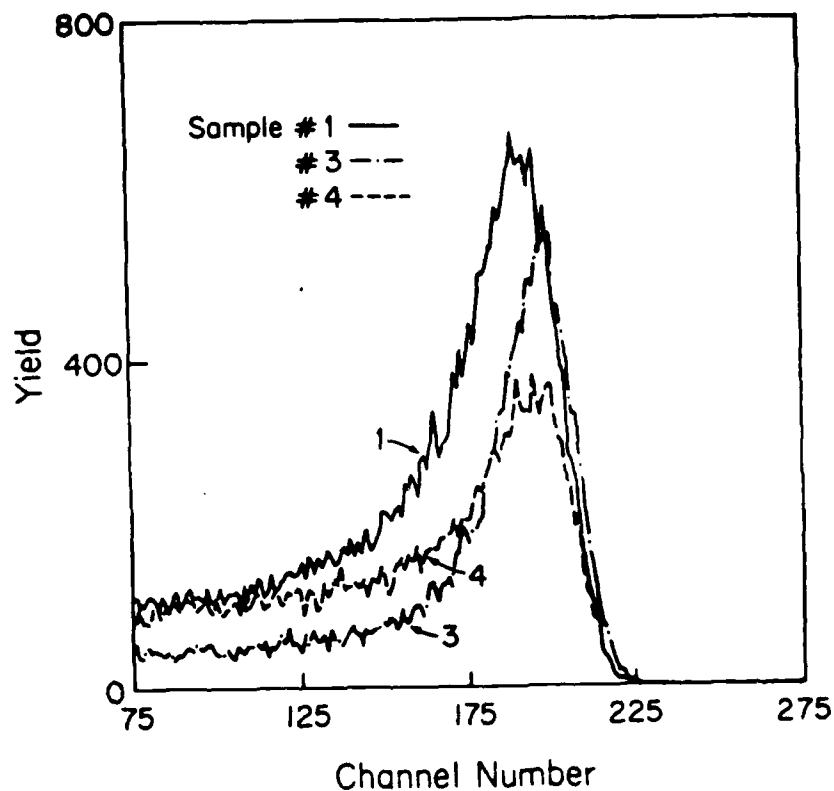


Fig. 3. Raman scattering spectra for three different Crystallume samples using a 150  $\mu$ m beam spot. The characteristic diamond frequency at 1332  $\text{cm}^{-1}$  is visible above a broad background

Raman scattering results for these samples showed the presence of the characteristic diamond frequency at 1332  $\text{cm}^{-1}$ , as illustrated in Figure 3. These results were obtained with low spatial resolution

(150 $\mu\text{m}$  spot), which in this case produced a broad asymmetric background peak, which is probably fluorescence due to an impurity. Microscopic examination showed that these samples were highly nonuniform. All three samples consisted of a uniform background (which showed no indication of diamond), spotted with a series of roughly circular "bull's eyes" with a visible ring structure (Fig.4). On sample #1 these features were typically ~ 100  $\mu\text{m}$  in diameter and were few in number. On the other two samples the "bull's eyes" were greater in number but smaller in diameter, typically 50 - 60  $\mu\text{m}$ . The "bull's eyes" apparently represent nucleation sites, as they showed strong diamond vibrations; high spatial resolution Raman spectra of all points examined on these features showed a peak at 1332  $\text{cm}^{-1}$  with FWHM of 9 - 13  $\text{cm}^{-1}$ , with no evidence of disordered carbon. The large widths recorded suggest that the diamond crystallites were small and rather strained.

### 3.3 General Electric Samples

The GE samples showed good quality diamond when examined by Raman scattering on both the top and the bottom (substrate side) surfaces. The average peak position was 1331.2  $\text{cm}^{-1}$  and the full width at half maximum (FWHM) varied from 3.9 to 5.1  $\text{cm}^{-1}$ , indicating that the examined parts of the film were of good crystal quality but not single crystals. These samples were cut by a laser beam from larger pieces. When a film was examined on the edges by optical reflectance microscopy, distinct layers were seen, as shown in Fig. 5 (right side). These layers appeared to be due to the effect of the laser cutting, since no such variation through the thickness of the film was observed at a cleaved edge (left side of Fig. 5). In confirmation of this observation, Raman scattering data obtained with the microbeam showed a strong diamond peak at 1332  $\text{cm}^{-1}$  for all depths on the cleaved edge (darkly circled spots on Fig. 5). However, for the laser-cut edge, only the top surface showed the strong diamond signal (Fig. 6, top spectrum), whereas the region near the bottom surface showed only a weak disordered carbon signal (Fig. 6, bottom spectrum).

Elastic recoil measurements taken on each surface of the G.E.

sample are shown in Fig. 7. The region near the top surface had a H concentration only equivalent to that of hydrocarbon contamination on the surface, whereas the region near the bottom surface contained 6 at% H.

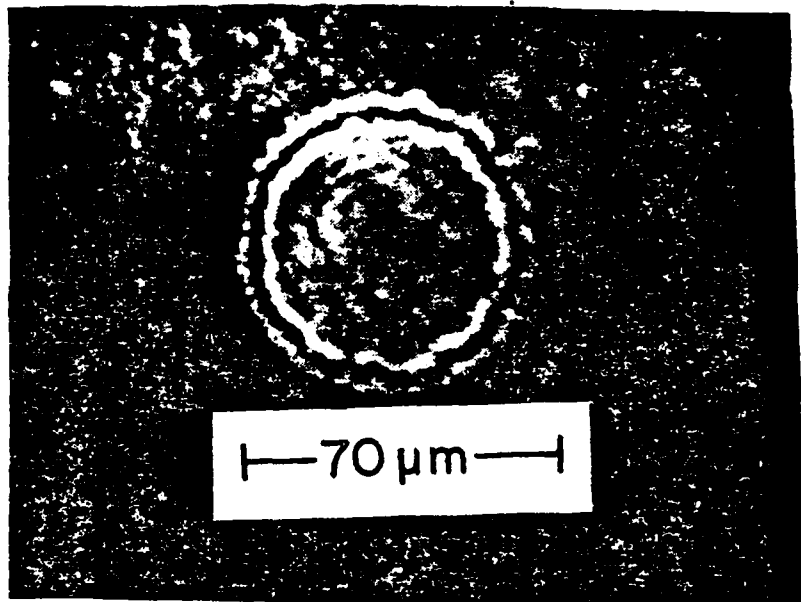


Fig. 4. Optical micrograph showing "bull's eye" ring structure on a Crystallume film.

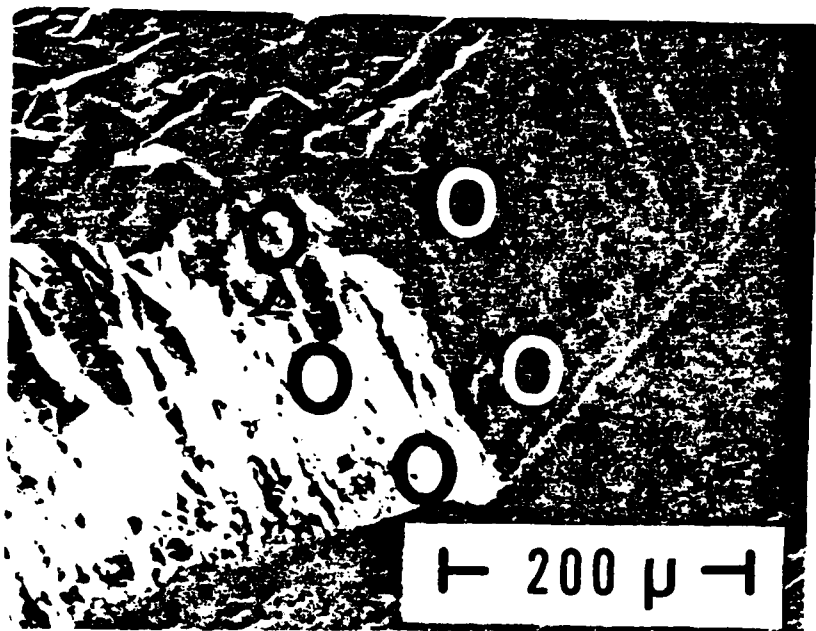


Fig. 5. Transverse optical micrograph of a G.E. diamond-like film, showing distinct layers on the right (laser cut) edge, but a uniform structure for the left (cleaved) edge.

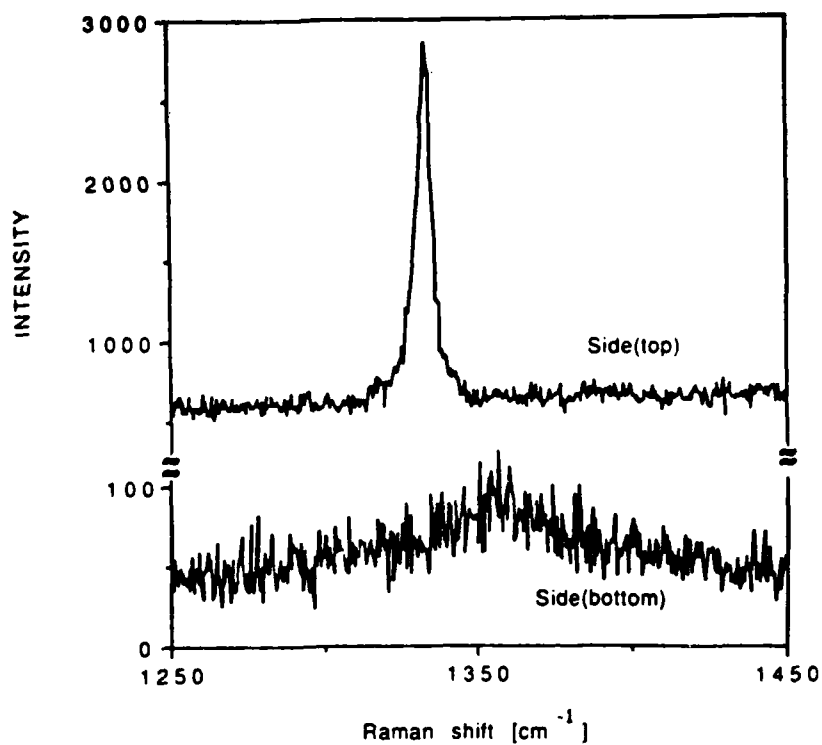


Fig. 6. Raman scattering spectra for a G.E. diamond-like film. The upper curve, taken at the top of the laser-cut edge (see Fig. 5), shows a strong  $1331 \text{ cm}^{-1}$  line, while the lower spectrum, taken at the lower part of that edge, shows a much broader line at about  $1360 \text{ cm}^{-1}$ .

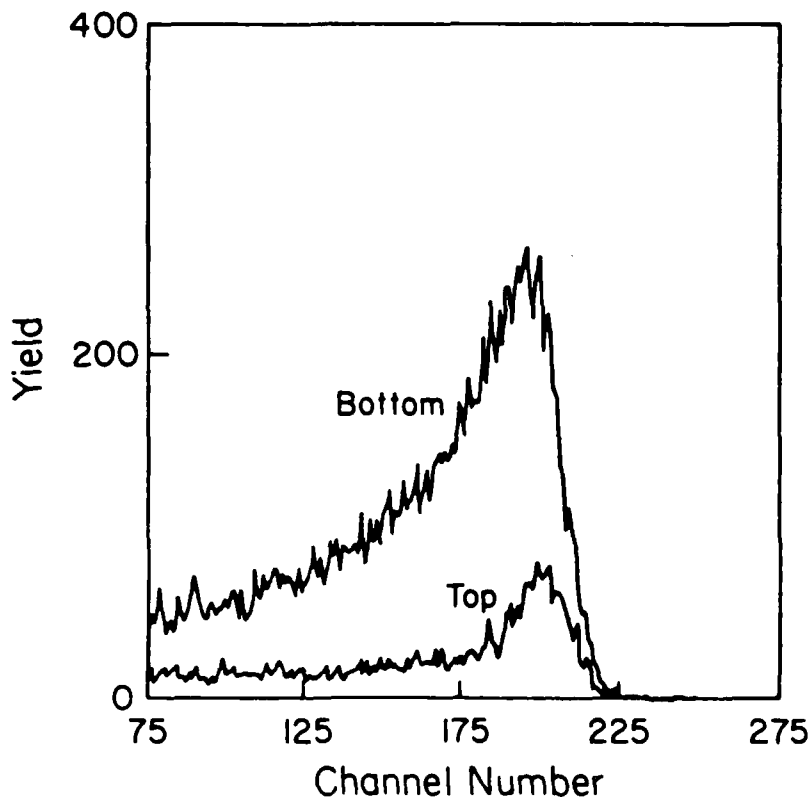


Fig. 7. Elastic recoil spectra recorded for the top and bottom surfaces of the G.E. sample of Figs. 5 and 6.

#### 4. DISCUSSION AND CONCLUSIONS

The present results have demonstrated that optical microscopy, elastic recoil detection spectroscopy and Raman scattering are a useful combination of techniques to characterize diamond-like films. Obvious surface and bulk features visible by microscopy were related to the H content by ERD and to the presence of true diamond material by Raman scattering.

#### 5. ACKNOWLEDGMENTS

The authors thank R.A. Rudder (RTI), S.H. Yokota (Crystallume Corp.) and T.R. Anthony (G.E. Co.) for supplying the diamond and diamond-like films.

This work is supported by the Office of Naval Research under contract N00014-87-K-0243.

#### 6. REFERENCES

1. Y. Saito, S. Matsuda and S. Nogita, *J. Mater. Sci. Letters* 5, 565 (1986).
2. M. Tsuda, M. Nakajima and S. Oikawa, *J. Amer. Chem. Soc.* 108, 5780 (1986).
3. Proc. 8th Int. Symp. on Plasma Chemistry, Tokyo 1987.
4. K. Kurihara, K. Sasaki, M. Kawarada and N. Koshino, *Appl. Phys. Lett.* 52, 437 (1988).
5. D.J. Vitkavage, R.A. Rudder, G.G. Fountain and R.J. Markunas, *J. Vac Sci. Technol.* A6, 1812 (1988).
6. A. Turos and O. Meyer, *Nucl. Instr. Meth.* B4, 92 (1984).
7. S.A. Solin and A.K. Ramdas, *Phys. Rev.* B1, 1687 (1970).
8. B.S. Elman, M.S. Dresselhaus, G. Dresselhaus, E.W. Maby, and H. Mazurek, *Phys. Rev.* B25, 4142 (1982).

PLASMA ASSISTED ETCHING OF DIAMOND

Wei-Kan Chu and G. Sandhu

Dept. of Physics & Astronomy

University of North Carolina at Chapel Hill

Diamond is the hardest material known to man and a reliable means of removing surface layers of diamond is of significant importance for microelectronics as well as for other applications such as polishing of the diamond surface.

There has been very little work done on the plasma assisted etching of diamond surfaces. Ion-beam-assisted etching of diamond using a  $Xe^+$  beam and a reactive gas flux of nitrogen dioxide ( $NO_2$ ) has been reported in the literature<sup>1</sup>. In addition, a study of the etching of diamond with argon and oxygen ion beams has been reported<sup>2</sup> in the literature. The sputtering yield for 500 eV oxygen ions was found to be seven times larger than that for 500 eV argon ions. But for 1000 eV oxygen and argon ions the corresponding ratio was only 2.5. This suggests that for higher energy oxygen ions the energy was deposited deep enough into the diamond that relatively inefficient etching was observed. The etching characteristics for 500 eV oxygen ion beams were apparently dominated by chemical interaction while for 1000 eV oxygen ions the etch yield was limited by the availability of energy required to remove CO and  $CO_2$  molecules in the near surface region.

We have done some preliminary studies on the possibility of using reactive ion etching (RIE) with  $O_2$  and  $H_2$  for the etching of diamond surfaces.

We have obtained etching rates of the order of 560<sup>o</sup>A/min for thin carbon films at room temperature using 400 eV oxygen ions. The same set-up has been used to obtain etching rates of 300 to 400<sup>o</sup>A/min for synthetic diamond samples procured from Crystallume Corp.

Figures 1 and 2 show the RBS spectra for a thin carbon film on a glass substrate before and after RIE in oxygen and hydrogen plasmas. The etch times were 3 and 2 minutes respectively. The conclusions from this set of experiments is summarized in the table below:

GAS	$\Delta H_f^*$	$\text{Log}_{10} W_f^{**}$	Ion Energy(keV)	Etch rate(A/minute)
O <sub>2</sub>	-26.4157(CO)	24.048	0.42	600-700
	-94.052(CO <sub>2</sub> )	68.091		350-400 (diamond)
H <sub>2</sub>	-17.889(CH <sub>4</sub> )	8.899	0.38	316

\*-Standard Heat of Formation at 25<sup>o</sup>C, K-cal/gmole.

\*\*-equilibrium const. for the reaction for forming given substance from its elements at 25<sup>o</sup>C.

As seen from the table, the trend in the etch rate is in broad agreement with the heats of formation and reaction rates of carbon with different gases.

#### Future Scope of the Work:

In order to increase the etching rate further, the possibility of heating the substrate and using gases like fluorine needs to be explored. Judging from the reaction rate and the heat of formation of  $CF_4$ , the etching rate is expected to be higher than in the case of  $O_2$ . We are also planning a set of experiments using an argon-oxygen gas mixture for RIE of diamond surfaces.

Synchrotron radiation-induced etching of a carbon film in an oxygen gas ambient has been studied<sup>3</sup>. It was concluded that the etching proceeds through nonthermal surface photochemical reactions induced by excitation of the carbon surface and/or adsorbed layers. This suggests that there is a strong possibility of obtaining enhancement in the etch rate by illuminating the diamond surface with UV light while etching in the RIE system.

#### REFERENCES:

1. N.N. Efremov, M.W. Geis, D.C. Flanders, G.A. Lincoln, and N.P. Economou, J.Vac.Sci Technol. B3 (1), 416 (1985).
2. Timothy J. Whetten, Angela A. Armstead, Thomas A. Grzybowski, and Arthur L. Ruoff, J.Vac.Sci. Technol. A2 (2), 477 (1984).
3. Hakaru Kyuragi and Tsuneo Urisu, Appl. Phys. Lett. 50 (18), 1254 (1987).

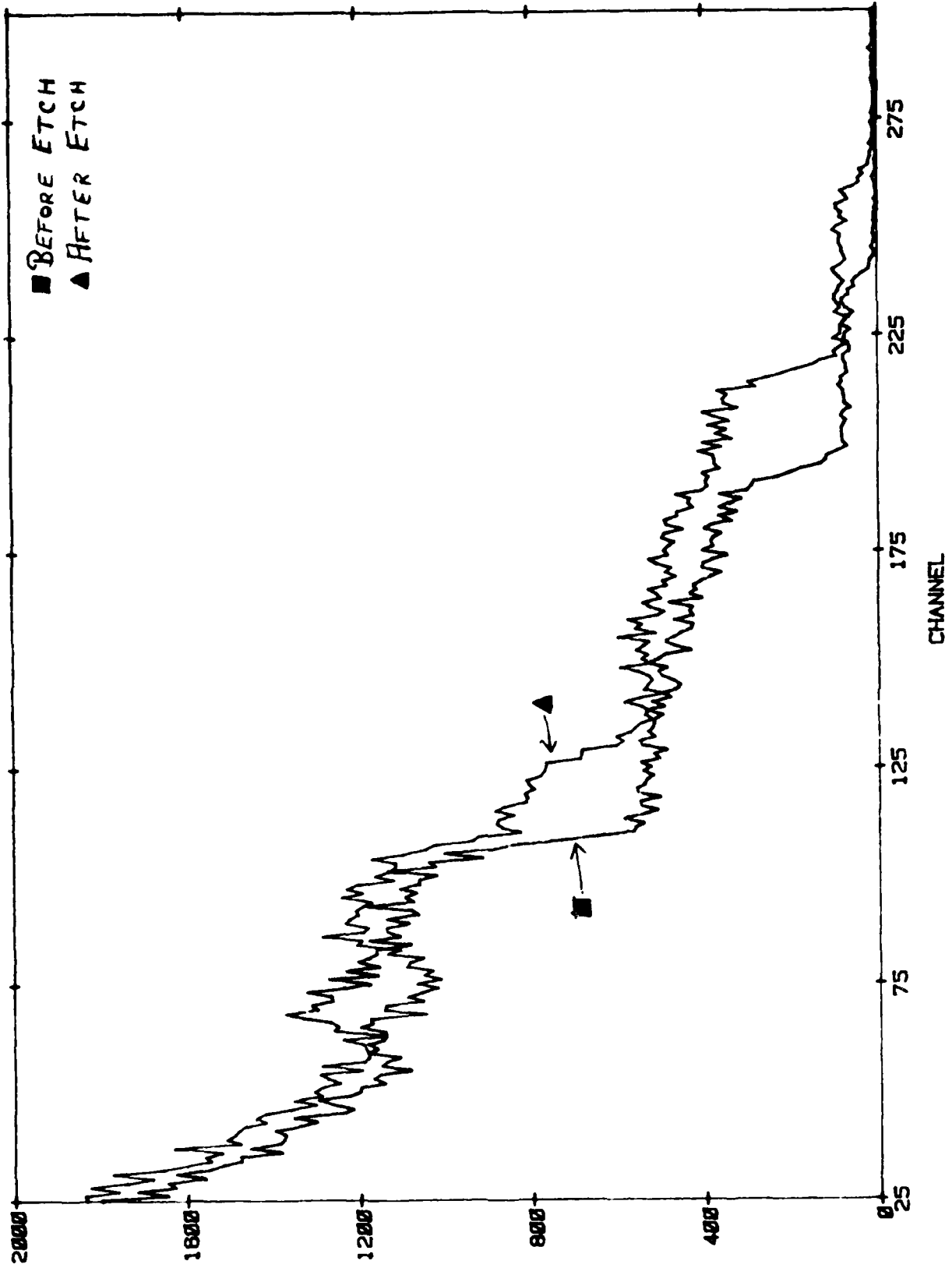


Fig. 1

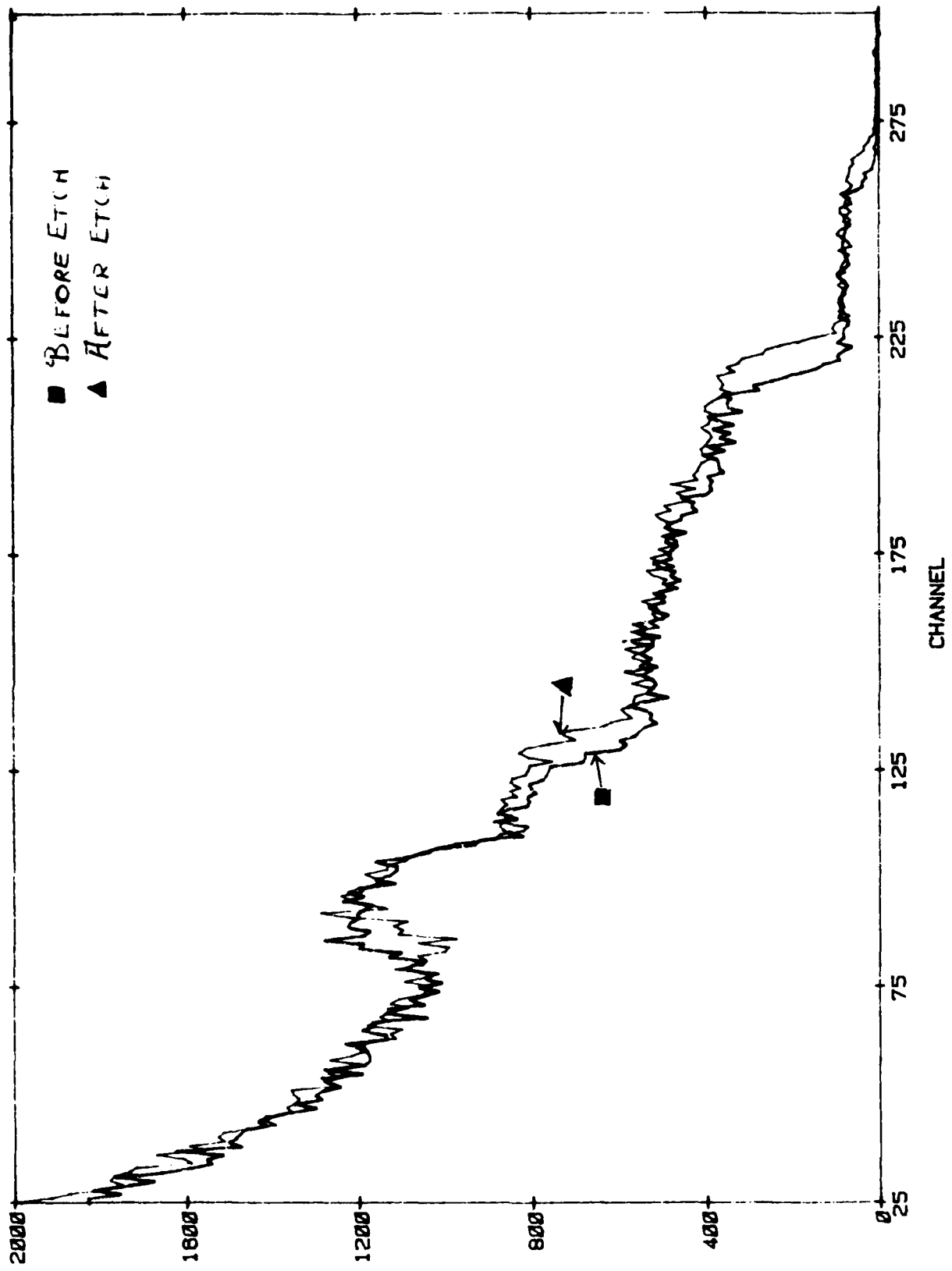


Fig. 2

## INCREASE IN GOLD-DIAMOND ADHESION BY ARGON SPUTTERING OF DIAMOND

### I. Introduction

The chemical inertness of diamond causes poor adhesion of metal films to diamond. This problem is particularly acute with gold films which are of considerable interest since they have potential use in electrodes when using diamonds for microelectronic applications, as well as for mechanical attachment of diamonds to various other metals and alloys.

The problem of attaching gold films to diamonds has been partially solved, for limited applications, by having a refractory metal film, such as tungsten, tantalum, or titanium, between the diamond and the gold. The bonding of the refractory metal to the diamond takes place by heating the diamond at several hundred degrees centigrade, thereby producing a refractory metal carbide which improves the bonding. Even the heat treatment does not always produce a mechanically stable bond between the diamond and the metal films.

We are working on procedures for improving the adhesion of gold to diamond without any heat treatment. The key idea is based on the formation of carbon bonds on the surface of the diamond by argon sputtering prior to depositions of the gold film. This process is derived from ion beam mixing and ion beam damage.

This report covers the results of two experiments designed to test the change in gold adhesion to diamond by ion mixing after deposition of the gold and by argon sputtering prior to deposition of the gold film. Both experiments were conducted on the same surface of the same diamond.

### II. Ion Mixing Experiment

A 1,000 angstrom gold film on diamond was implanted with 2 MeV helium ions in five different regions, with the integrated flux in each region being different, with a maximum of approximately  $5 \times 10^{15}/\text{cm}^2$ . The beam was triangular shaped, approximately 1 mm x 1 mm x 1 mm.

The adhesion of the gold film was tested by using the "Scotch Tape Test," which consisted of pressing the tape to the gold film and then removing the tape. The gold film was removed by this test so there was no apparent improvement in adhesion by the ion mixing at the gold-diamond interface.

### III. Sputtering of Argon Ions Prior to Sputtering of Gold Film

#### A. Experimental Conditions

The diamond was masked with a diamond film (10 mm x 10 mm x 0.4 mm), which had been given the same cleaning procedure as the diamond. The mask was placed so that only a part of the diamond surface was exposed to the sputtering by argon ions. The diamond and the mask were placed in the specimen holder so that no holder material would be sputtered onto the diamond during the argon sputtering.

#### B. Argon Sputtering Prior to Deposition of Gold

The specimen holder was placed at the target position in a sputtering chamber. The argon beam was focused to approximately 8 mm diameter so the the beam sputtered only the diamond and a small region of the holder. The argon beam was 0.5 milliamps at 14 keV and had a duration of 98 minutes. The chamber pressure was  $4.2 \times 10^{-4}$  torr during this argon sputtering cleaning.

At conclusion of the argon sputtering, an argon pressure (above atmosphere) was maintained in the chamber and the specimen holder's position was replaced a large piece of high purity gold. The diamond film mask was removed from the specimen holder, and the holder was placed so that the subsequently sputtered gold would form a film on the whole diamond surface. These operations were performed without exposing the deposition chamber and its contents to air.

### C. Gold Sputtering

The gold was sputter for six hours at a rate of approximately 150 A per hour with the argon beam at 13.5 keV and a current of 0.25 milliamps. The chamber pressure was  $5.4 \times 10^{-5}$  torr throughout the deposition.

## V. Visual Differences Produced by Argon Sputtering

### A. Microscopic Examination: Dark Field Illumination

There were obvious differences in the appearances of the gold films in the argon cleaned region and the non-argon sputtered region. As well being able to observe the step produced by the argon beam's sputtering away a thin layer of the diamond, the gold film in the argon sputtered region was more uniform and had a slight different color which, as subsequently shown, was caused by the non-argon sputtered region gold film not being as smooth.

A microscopic examination with dark field illumination revealed a marked difference between the gold films in the non-argon sputtered region and the argon sputtered region. The first region's gold film was not uniform and characterized by a patina surface in some regions, and that patina ended abruptly where the argon cleaned region began. The sputtered region had a gold film which was smooth, with no flaws observed.

### B. Scanning Electron Microscope

The two regions were studied with a scanning electron microscope. The gold film on the uncleaned region had a distinctive matted structure, with the "mounds" being approximately 0.2 microns wide and less than 0.2 microns high. On the other hand, it was not possible to discern any structure in the gold films in the argon cleaned region so any surface variations would have to have been less than the approximately 1000 angstroms resolution for the SEM parameters used for these observations.

## VI. Scotch Tape Test

Scotch Tape was pressed onto the gold film and removed. Care was taken to be certain that all of the film was covered by the tape prior to removing the tape. This procedure was carried out under a microscope to insure that good tape-film contact had been made. This procedure was repeated several times. The result was that the gold film was removed only in the unsputtered region. When the film was removed in that region, the gold film broke near the demarcation of the unsputtered-sputtered region. No gold was removed from the region sputtered with argon prior to deposition of the gold film.

## VII. Conclusion

Whereas ion mixing did not increase the gold film's adhesion to the diamond surface, there was a substantial improvement in the adhesion of sputtered gold films to that same surface when the diamond is sputtered with argon ions prior to deposition of the gold and the diamond is kept in an argon atmosphere during and between all sputtering processes. The differences in structure and adhesion of the gold on the unsputtered and sputtered areas are shown in the following figures.

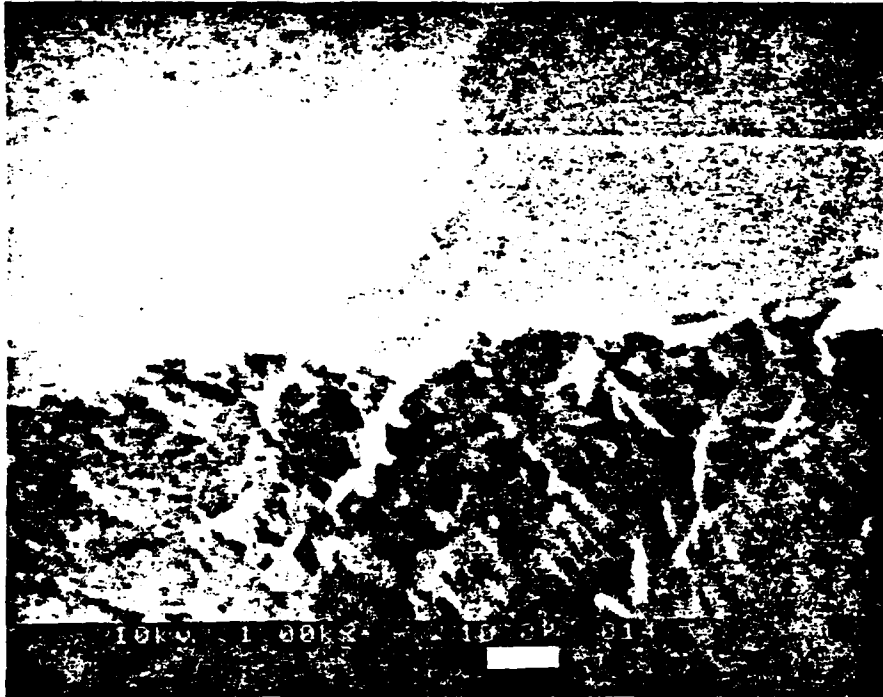


Fig. 1 SEM photograph of gold film on argon sputtered diamond. Left side was not sputtered with argon; right side was sputtered with argon. The gold film on the right was smooth and uniform.



Fig. 2 SEM photograph of gold film on unsputtered area. The film was characterized by "mounds" with width and heights of approximately 1,000 angstroms. It was not possible to resolve any structure in the film in the sputtered area.

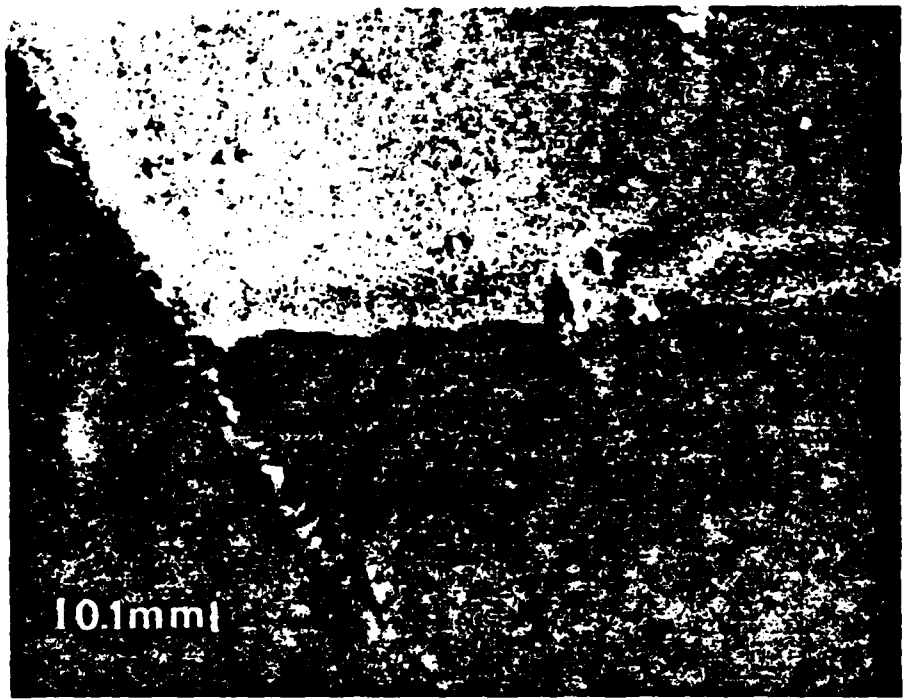


Fig. 3 Dark field illumination of gold film on unspattered area (top) and sputtered area (bottom). The gold film in the sputtered area had no light scattering regions.

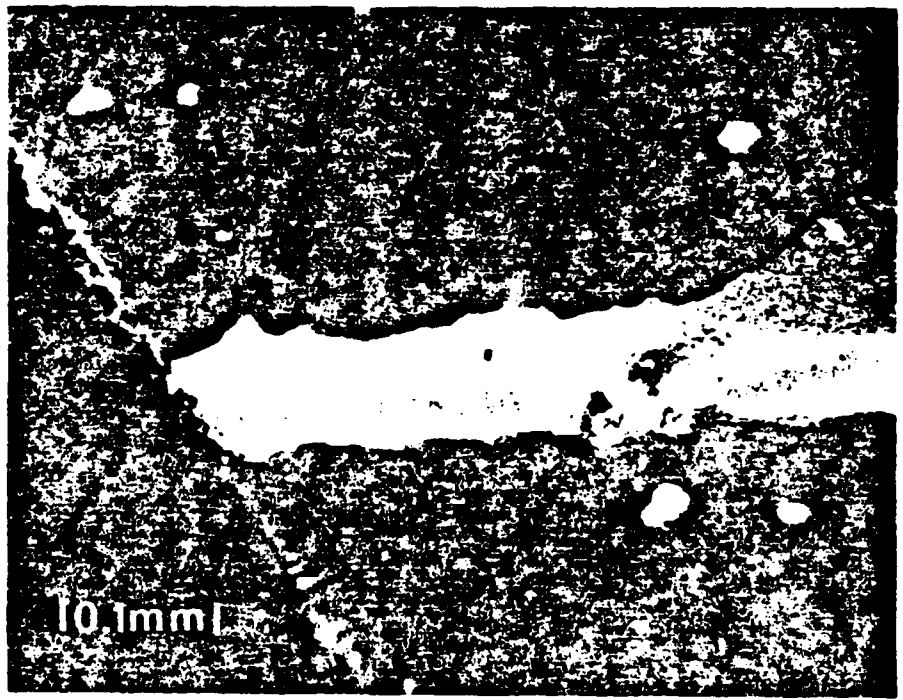


Fig. 4 Same as Fig. 3 after "Scotch Tape" test. The gold film was partially removed in the unspattered area (top) whereas it remained in the sputtered area (bottom).

## INCREASE IN GOLD-DIAMOND ADHESION BY ARGON SPUTTERING OF DIAMOND

### I. Introduction

The chemical inertness of diamond causes poor adhesion of metal films to diamond. This problem is particularly acute with gold films which are of considerable interest since they have potential use in electrodes when using diamonds for microelectronic applications, as well as for mechanical attachment of diamonds to various other metals and alloys.

The problem of attaching gold films to diamonds has been partially solved, for limited applications, by having a refractory metal film, such as tungsten, tantalum, or titanium, between the diamond and the gold. The bonding of the refractory metal to the diamond takes place by heating the diamond at several hundred degrees centigrade, thereby producing a refractory metal carbide which improves the bonding. Even the heat treatment does not always produce a mechanically stable bond between the diamond and the metal films.

We are working on procedures for improving the adhesion of gold to diamond without any heat treatment. The key idea is based on the formation of carbon bonds on the surface of the diamond by argon sputtering prior to depositions of the gold film. This process is derived from ion beam mixing and ion beam damage.

This report covers the results of two experiments designed to test the change in gold adhesion to diamond by ion mixing after deposition of the gold and by argon sputtering prior to deposition of the gold film. Both experiments were conducted on the same surface of the same diamond.

### II. Ion Mixing Experiment

A 1,000 angstrom gold film on diamond was implanted with 2 MeV helium ions in five different regions, with the integrated flux in each region being different, with a maximum of approximately  $5 \times 10^{15}/\text{cm}^2$ . The beam was triangular shaped, approximately 1 mm x 1 mm x 1 mm.

The adhesion of the gold film was tested by using the "Scotch Tape Test," which consisted of pressing the tape to the gold film and then removing the tape. The gold film was removed by this test so there was no apparent improvement in adhesion by the ion mixing at the gold-diamond interface.

### III. Sputtering of Argon Ions Prior to Sputtering of Gold Film

#### A. Experimental Conditions

The diamond was masked with a diamond film (10 mm x 10 mm x 0.4 mm), which had been given the same cleaning procedure as the diamond. The mask was placed so that only a part of the diamond surface was exposed to the sputtering by argon ions. The diamond and the mask were placed in the specimen holder so that no holder material would be sputtered onto the diamond during the argon sputtering.

#### B. Argon Sputtering Prior to Deposition of Gold

The specimen holder was placed at the target position in a sputtering chamber. The argon beam was focused to approximately 8 mm diameter so the the beam sputtered only the diamond and a small region of the holder. The argon beam was 0.5 milliamps at 14 keV and had a duration of 98 minutes. The chamber pressure was  $4.2 \times 10^{-4}$  torr during this argon sputtering cleaning.

At conclusion of the argon sputtering, an argon pressure (above atmosphere) was maintained in the chamber and the specimen holder's position was replaced a large piece of high purity gold. The diamond film mask was removed from the specimen holder, and the holder was placed so that the subsequently sputtered gold would form a film on the whole diamond surface. These operations were performed without exposing the deposition chamber and its contents to air.

### C. Gold Sputtering

The gold was sputter for six hours at a rate of approximately 150 A per hour with the argon beam at 13.5 keV and a current of 0.25 milliamps. The chamber pressure was  $5.4 \times 10^{-5}$  torr throughout the deposition.

## V. Visual Differences Produced by Argon Sputtering

### A. Microscopic Examination: Dark Field Illumination

There were obvious differences in the appearances of the gold films in the argon cleaned region and the non-argon sputtered region. As well being able to observe the step produced by the argon beam's sputtering away a thin layer of the diamond, the gold film in the argon sputtered region was more uniform and had a slight different color which, as subsequently shown, was caused by the non-argon sputtered region gold film not being as smooth.

A microscopic examination with dark field illumination revealed a marked difference between the gold films in the non-argon sputtered region and the argon sputtered region. The first region's gold film was not uniform and characterized by a patina surface in some regions, and that patina ended abruptly where the argon cleaned region began. The sputtered region had a gold film which was smooth, with no flaws observed.

### B. Scanning Electron Microscope

The two regions were studied with a scanning electron microscope. The gold film on the uncleaned region had a distinctive matted structure, with the "mounds" being approximately 0.2 microns wide and less than 0.2 microns high. On the other hand, it was not possible to discern any structure in the gold films in the argon cleaned region so any surface variations would have to have been less than the approximately 1000 angstroms resolution for the SEM parameters used for these observations.

## VI. Scotch Tape Test

Scotch Tape was pressed onto the gold film and removed. Care was taken to be certain that all of the film was covered by the tape prior to removing the tape. This procedure was carried out under a microscope to insure that good tape-film contact had been made. This procedure was repeated several times. The result was that the gold film was removed only in the unsputtered region. When the film was removed in that region, the gold film broke near the demarcation of the unsputtered-sputtered region. No gold was removed from the region sputtered with argon prior to deposition of the gold film.

## VII. Conclusion

Whereas ion mixing did not increase the gold film's adhesion to the diamond surface, there was a substantial improvement in the adhesion of sputtered gold films to that same surface when the diamond is sputtered with argon ions prior to deposition of the gold and the diamond is kept in an argon atmosphere during and between all sputtering processes. The differences in structure and adhesion of the gold on the unsputtered and sputtered areas are shown in the following figures.

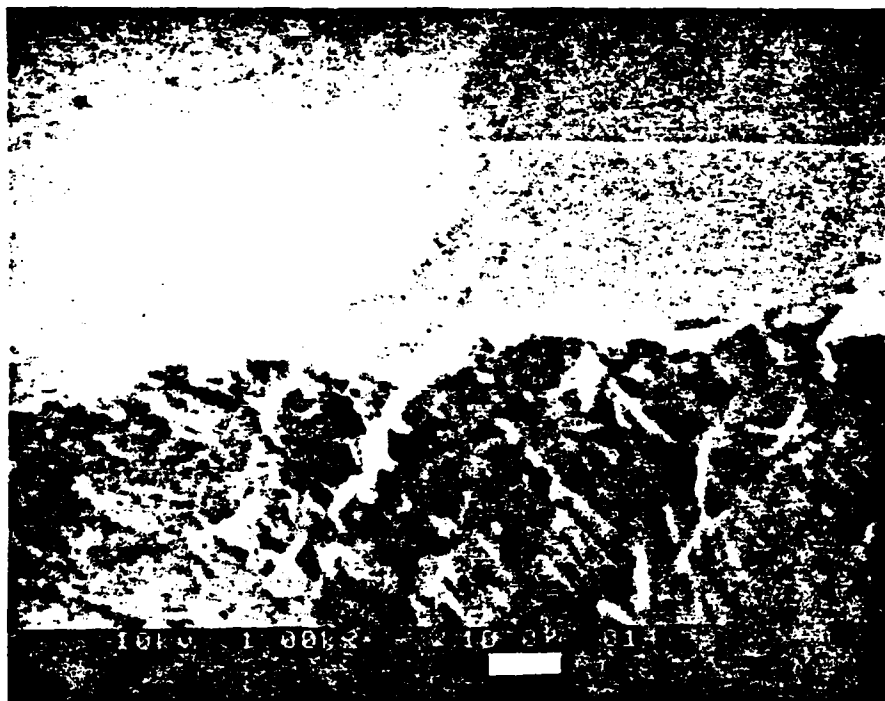


Fig. 1 SEM photograph of gold film on argon sputtered diamond. Left side was not sputtered with argon; right side was sputtered with argon. The gold film on the right was smooth and uniform.

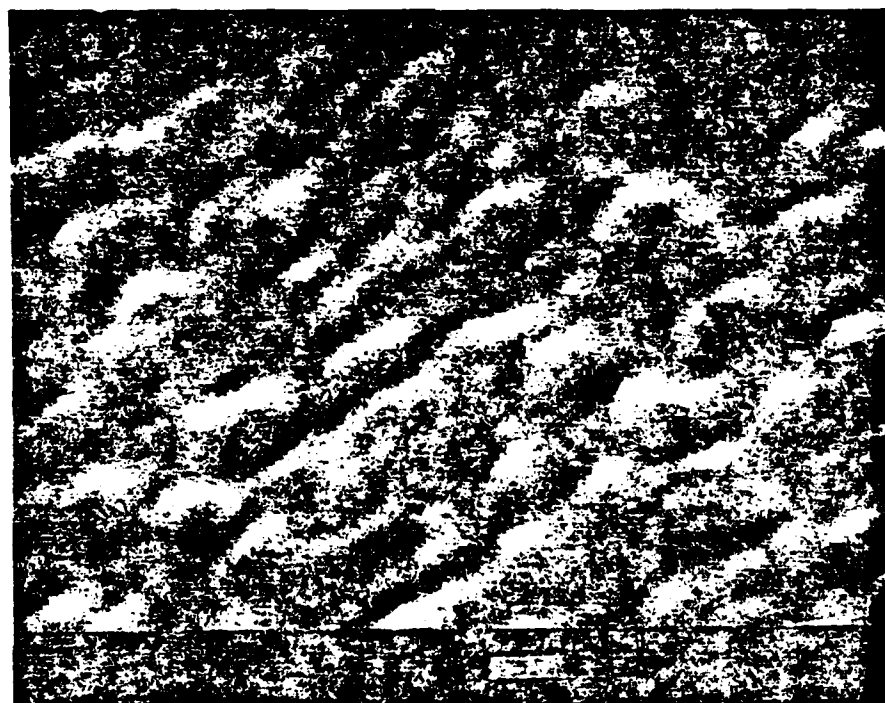


Fig. 2 SEM photograph of gold film on unsputtered area. The film was characterized by "mounds" with width and heights of approximately 1,000 angstroms. It was not possible to resolve any structure in the film in the sputtered area.

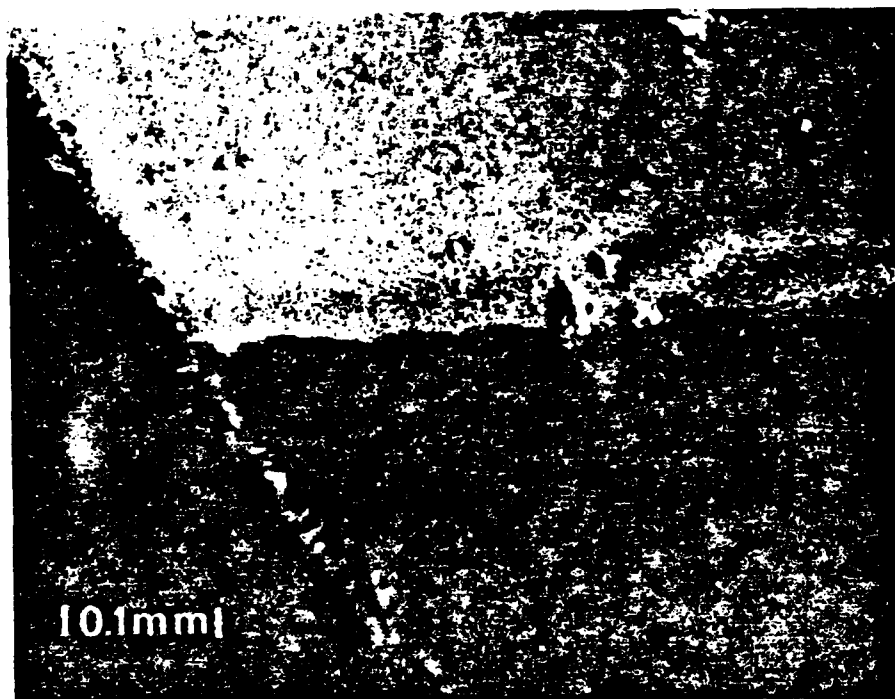


Fig. 3 Dark field illumination of gold film on unspattered area (top) and spattered area (bottom). The gold film in the spattered area had no light scattering regions.

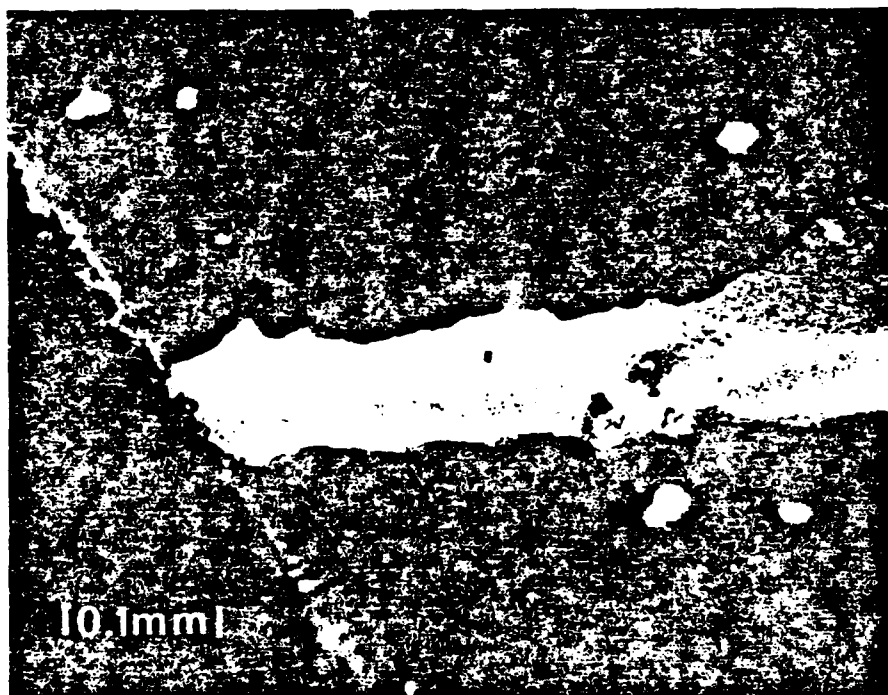


Fig. 4 Same as Fig. 3 after "Scotch Tape" test. The gold film was partially removed in the unspattered area (top) whereas it remained in the spattered area (bottom).